

# Simulation of LCM Processes with Cellular Automats

Prof. Dr. Markus Henne

## Abstract

Finite Element Methods (FEM) are at present available for simulating resin injection processes. However, they are extremely time-consuming, and even then they demand excessive computing power if an iterative process is used for optimising the injection parameters; furthermore, the quantitative predictions of the filling time and the evolution of the pressure during the filling of the mould are very inaccurate. For these reasons FEM-based simulation is scarcely ever used in practice.

In the work described here a cellular automat is used to simulate the injection process. The algorithm calculates the pressure in a cell from the pressures in the neighbouring cells and from the properties of the cell. It takes account of all the factors that have an influence, such as permeability, porosity and the geometry of the cavity. It is tuned to give a picture of the mould-filling that is as realistic as possible, using experimental results and values based on experience.

Essentially the algorithm correctly represents the filling process. In particular the effects of the local permeability and porosity of the material are realistically portrayed.

It is also possible to simulate correctly the effect of several independently switched injection points.

On the other hand there is room for improvement in considering different cell densities and in taking account of the cavity dimensions.

## 1. Introduction

Liquid Composite Moulding (LCM) covers a class of manufacturing processes of high-quality fibre reinforced composites for the most demanding applications. These are resin injection processes in which the dry fibre structure is placed in the die cavity where it is soaked in the resin-hardener mixture, after which the die is closed and the component is cured under high temperature and pressure.

Figure 1 shows schematically the sequence of process steps. The textile fibre material is cut to size, coated with a thermoplastic binder and then warmed up. The pliable mat is then formed in a die and cooled down, after which the now rigid fibre structure is ejected from the die. After any necessary finishing steps such as edge trimming, the blank is placed in the preheated injection mould. The mould is closed and evacuated, after which the resin-hardener mix is injected, filling every interstice of the mould and preform. After the required curing and cooling time the now solid component is removed from the mould. A final stage of tempering gives the component the required finished mechanical properties [1]. There follow any necessary finishing processes, and the component is ready for use.

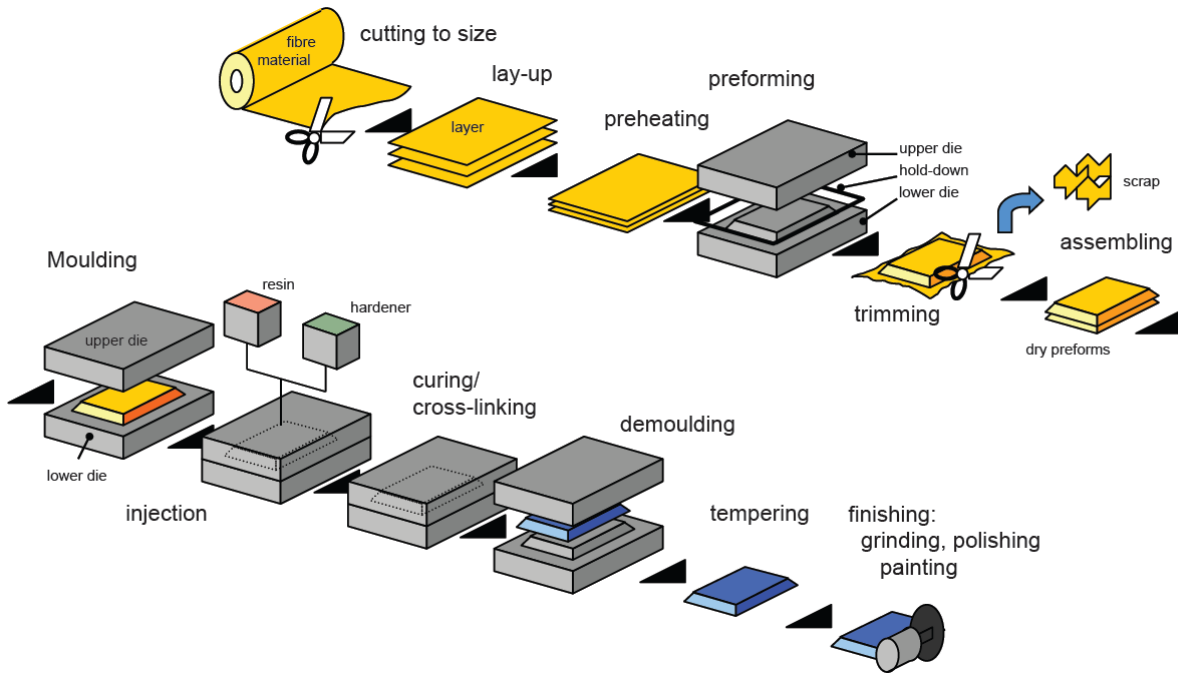


Figure 1: RTM Process

LCM processes are closed processes, i.e. during injection the mould cavity is open only to the liquid mix flowing in, and is otherwise inaccessible. For this reason it is difficult to follow the process of mould filling or to influence it in any way. At best, appropriately placed sensors can deliver a signal at the instant the filling front reaches them.

Suitable process control is decisive in ensuring process repeatability and the quality of the finished component. If either the injection points or the mould evacuation points are incorrectly chosen, then air pockets may occur, impairing product quality. Apart from this, the process should be laid out to achieve the shortest possible cycle time and hence the highest productivity.

The Finite Element Method (FEM) is today applied more and more often for optimising design and control of the process. The approach used in applying FEM to the calculation of the filling front in porous materials is based on Darcy's Law, which describes the behaviour of liquids flowing through porous materials. By experimenting with water flowing through porous materials, Henry Darcy (1803-1858) discovered his law, which describes a linear relationship between the flow rate and the pressure gradient for laminar flow. In the case considered here the flow velocity of the resin depends on the pressure distribution in the mould, the permeability of the fibre reinforcement and the viscosity of the resin.

$$v = \frac{K}{\eta} \cdot \nabla p \quad (1)$$

- $v$  Flow velocity of the resin
- $\eta$  Viscosity of the resin
- $K$  Permeability of the reinforcing fibres
- $\nabla p$  Pressure gradient

Simulation based on the Finite Element Method is however very expensive, and furthermore its quantitative prediction of filling time and the evolution of the pressure distribution is very inaccurate; for these reasons it is seldom used in practice. Moreover, the method seldom takes into account thermal effects, which in resin injection processes can have a decisive influence.

On top of all this, the algorithms available today for efficient iterative optimisation of the process require too much computing power. A single run can, depending on the number of elements and the geometrical complexity of the component, take from a few minutes to several hours. Consequently, an optimisation that may require from several hundreds to some thousands of iterations takes much time and may be in fact impracticable because of limited computing capacity.

A new approach to the simulation of resin injection processes is taken in this study, based on the idea of cellular automats. Numerical simulations using cellular automata require in many cases far fewer calculations and can therefore very substantially reduce the time required.

## 2. Cellular Automats

Cellular Automats were first proposed in 1940 by John von Neumann, Stanislaw Ulam und Alan Turing at Los Alamos [2]. They are valid for spatially discrete time-dependent systems, in which the state of an individual cell at a given time step depends primarily upon its own state and those of the cells in a predefined neighbourhood at the end of the previous step. In order that cellular automats may be used to simulate physical phenomena that are described by sets of differential equations, they must be approximated either by the top-down or by the bottom-up method.

In the top-down method the cellular automat is derived from the differential equation that governs the behaviour of the object itself. In the bottom-up approach on the other hand the cellular automat is programmed so as to ensure that its behaviour corresponds purely and simply to that observed in the real system.

In the case under consideration a middle way is preferred, whereby in the bottom-up approach the algorithm is based on the influence of the individual parameters according to Darcy's law. The cellular automat presented here was developed specifically for hollow shell-shaped components – "2½ dimensional" – which is often the form of fibre-reinforced plastic structures, though the algorithm can in principle also be used for true three-dimensional structures.

The algorithm calculates the state of the pressure distribution in a cell during filling from the pressure in the cell itself as well as that in the neighbouring cells, and from the properties of the cells in that region at that time, according to:

$$p_{t+1} = p_t + \left(\frac{K}{\bar{K}}\right)^q \cdot \frac{1}{m} \cdot \sum_{i=1}^m \left(\frac{d_i \cdot \phi_i}{d \cdot \phi}\right)^r \cdot \left(\frac{\bar{l}}{l_i}\right)^s \cdot (p_{i,t} - p_t) \quad (2)$$

$p$	Pressure of the cell	[N/ m <sup>2</sup> ]
$\bar{K}$	Average permeability	[m <sup>2</sup> ]
$d$	Height of the cavity	[m]
$\phi$	Porosity	[-]
$l$	Distance to the neighbouring cell	[m]
$\bar{l}$	Average distance between cells	[m]
$q, r, s$	Weighting factors	[-]
$m$	Number of neighbouring cells taken into account	[-]

A boundary condition is that the pressure in a cell may never exceed that at the point of injection.

This algorithm allows for the effects of all the influential factors such as permeability, viscosity and cavity height. These parameters are normalised according to the prevailing conditions, and weighted by the factors  $q$ ,  $r$  and  $s$ .

The parameter  $m$  prescribes the number of neighbouring cells to be taken into account in calculating the pressure, i.e. the same number of neighbours is always used, irrespective of the cell density.

In this form the algorithm is formulated for isotropic permeability  $K$ . The effect of anisotropy – which anyway has a subordinate effect in real components – can if need be allowed for by an extension of the cellular automat.

All the influential parameters, including cell spacing, cavity height and porosity are normalised. The term with exponent  $r$  adjusts the weight of the cell in relation to that of its neighbours, depending on their properties. The term with exponent  $s$  makes the cellular automat independent of the cell density, i.e. it ensures that irrespective of the cell density the filling behaviour is always the same for the same cell properties.

The weighting factors must be adjusted in order to obtain the best approximation to the real flow behaviour. The following values were selected for the present case:

$$q = 1$$

$$r = 1$$

$$s = 2$$

The injection point is determined, for which a constant pressure  $p_{inj}$  is allotted. The calculation starts, and this pressure extends throughout the surrounding cells. The pressure field is evaluated at each step of the calculation, and a decision made as to whether a given cell is to be considered as still dry or as filled with resin mix. The threshold criterion for complete filling of the cell is the partial vacuum pressure  $p_{vac}$ . That is to say, the cell is considered to be soaked with resin mix as soon as its pressure exceeds the partial vacuum pressure of evacuation of the mould cavity. It follows that for the simulation a cell can in this respect be in only one of two states: either completely dry, or else completely soaked with resin mix. Intermediate states obviously exist in reality, but in practice have little influence on the outcome.

An interesting and useful aspect of this approach is that it makes it possible to evaluate simply and elegantly the effect of the evacuation pressure on the filling behaviour.

Figure 2 illustrates graphically the steps in the calculation.

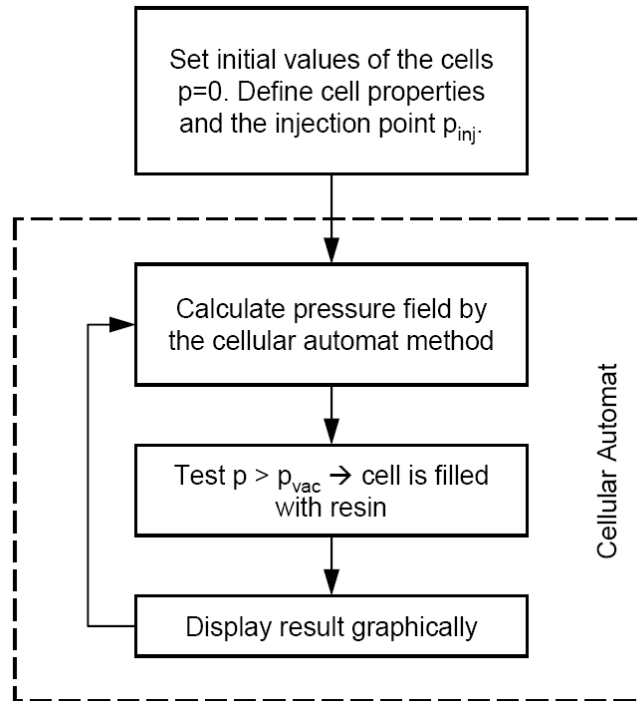


Figure 2: Schematic view of the stepwise calculation.

The simulation showed that an unrealistically large pressure drop occurred at the injection point, causing an unrealistically low pressure distribution in the cells (Figure 3).

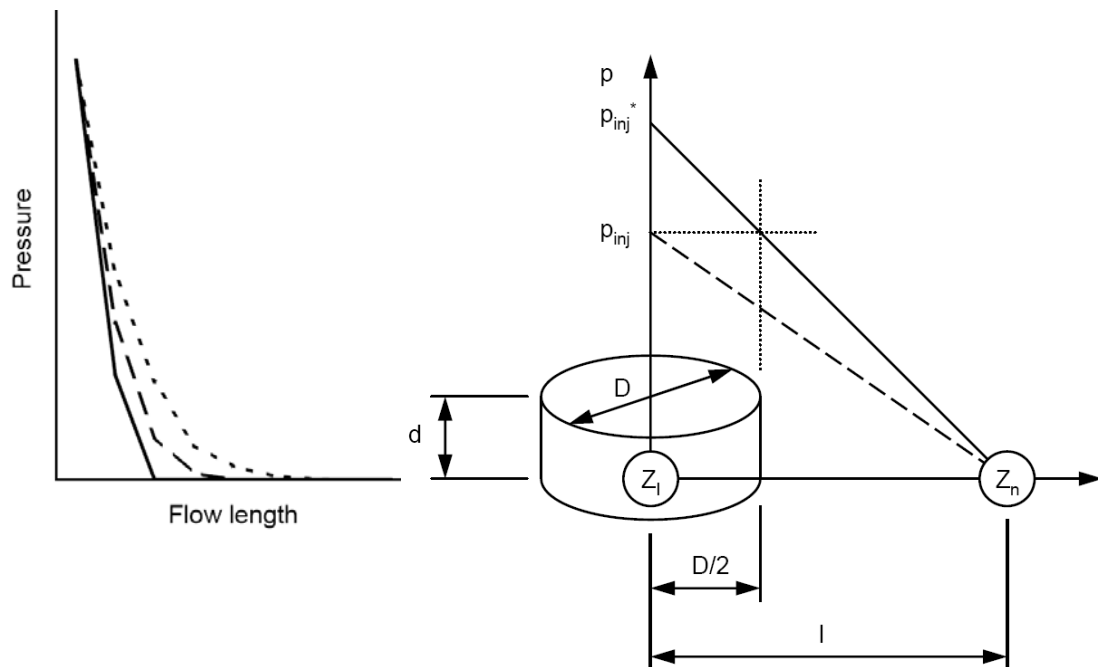


Figure 3: Typical development of the pressure distribution from the injection point to the filling front (left) and pressure conditions around the injection point (right).

The reason for this is the assumption of a point injection, i.e. a hole of zero diameter. In reality, the inlet is a drilling, so that there is constant injection pressure over a circular section of radius  $D/2$  at the cell defined as the inlet point. To allow for this, the injection pressure  $p_{inj}$  is corrected upwards so as to maintain at least the injection pressure over the whole of the circular surface of the cell where the injection takes place.

$$p_{inj}^* = \frac{p_{inj} \cdot \bar{l}}{(\bar{l} - D/2)} \text{ whereas } D/2 < \bar{l} \quad (3)$$

$p_{inj}$	Injection pressure in the inlet	[N/ m <sup>2</sup> ]
$p_{inj}^*$	Corrected injection pressure	[N/ m <sup>2</sup> ]
$D$	Diameter of the inlet	[m]

In order to obtain quantitative predictions of the progress of mould filling the algorithm must be applied at discrete time steps, which are held constant over the whole of the time to fill the mould. The calculated pressure falls off exponentially in the direction of the filling front, as does the pressure gradient. This means that the filling velocity may be expected to fall off as the mould fills.

Equation 4 describes the approach to calculating the time step; it is based on Darcy's Law.

$$v = \frac{\Delta f}{\Delta t} = \frac{K}{\eta} \nabla p \approx \frac{K}{\eta} \cdot \frac{\Delta p}{\Delta l} \rightarrow \Delta t = \frac{\eta \cdot \Delta l \cdot \Delta f}{K \cdot \Delta p} \sim \frac{\eta \cdot l_{typ} \cdot \bar{l}}{\bar{K} \cdot (p_{inj} - p_{vac})} \quad (4)$$

$\Delta t$	Discrete time step	[s]
$\Delta f$	Flow distance per time step	[s]
$l_{typ}$	Typical length of the model	[m]

A typical length is the square root of the surface area of the model:

$$l_{typ} = \sqrt{A} \approx \sqrt{n} \cdot \bar{l} \quad (5)$$

$A$	Surface area of the model / part	[m <sup>2</sup> ]
$n$	Total number of cells in the model	[-]

For a given example an appropriate time step can be calculated in this way in real time, which makes it possible to predict the evolution of mould filling in time.

### 3. Evaluation and Interpretation

In a test programme, individual parameters of the cellular automat are adjusted and the resulting filling pattern is displayed graphically. The test component is a square plate 500 mm x 500 mm, and is divided into nine equal square elements, whose properties can be

individually varied. Increases in permeability in the edge zones (which occur in reality) are not taken into account in the model.

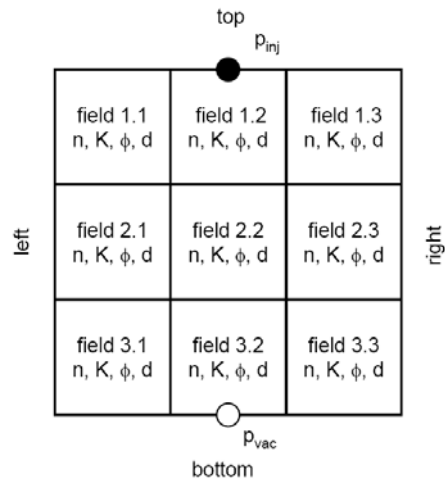


Figure 4: Composition of the simulation field

The following values are taken as standard:

$$\begin{aligned}
 m &= 8 \\
 n &= 441 \\
 D &= 0.01m \\
 p_{inj} &= 5bar \\
 p_{vac} &= 0.1bar \\
 K &= 2 \cdot 10^{-9} m^2 \\
 \phi &= 0.5 \\
 d &= 0.002m \\
 \eta &= 100mPas
 \end{aligned}$$

The various fill states of the cells are classified as dry, under pressure, and soaked (Figure 5). As explained above, a cell is considered to be soaked when its pressure is higher than the partial vacuum pressure  $p_{vac}$ . This limitation has the effect of making the development of the filling front independent of the geometrical spreading of the pressure field.

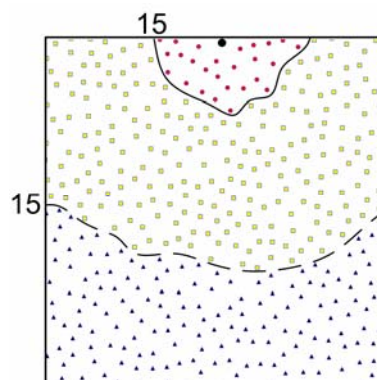


Figure 5: Graphical evaluation after fifteen steps  
Solid line – flow front, broken line – pressure front

The individual factors are systematically varied in the way described in Table 1.

Variation	Description
Distribution of the cells	Comparison of the results for a uniform distribution of the cells with those for an arbitrary distribution, the total number of cells being the same in both cases
Note: In the remaining cases only arbitrary cell distribution is used in the model.	
Inlet position	Qualitative behaviour for inlet placed in the middle of a side, at a corner and in the middle of the field
Injection pressure	Effect of doubling or halving the injection pressure (pressure held constant during filling)
Cell density	Variation of the cell density in the direction of injection and at right angles to it. Cell density declining stepwise from left to right (A), from top to bottom (B) or from bottom to top (C)
Permeability	Variation of the permeability in the direction of injection and at right angles to it. Permeability declining stepwise from left to right (A), from top to bottom (B) or from bottom to top (C)
Porosity	Variation of the porosity in the direction of injection and at right angles to it. Porosity declining stepwise from left to right (A), from top to bottom (B) or from bottom to top (C).
Cavity height	Variation of the cavity height in the direction of injection and at right angles to it. Cavity height declining stepwise from left to right (A), from top to bottom (B) or from bottom to top (C).

Table 1: Test programme

Example: Figure 6 shows the pattern of variation for permeability.

K	K	K	2K	K	0.5K	2K	2K	2K	0.5K	0.5K	0.5K
K	K	K	2K	K	0.5K	K	K	K	K	K	K
K	K	K	2K	K	0.5K	0.5K	0.5K	0.5K	2K	2K	2K
Starting Position			Case A			Case B			Case C		

Figure 6: Variation of permeability.

The results are illustrated and described in the following figures 7 to 13 and the associated text. The numbers show the number of calculation steps after the start of injection. The solid line is the flow front and the broken line the pressure front.



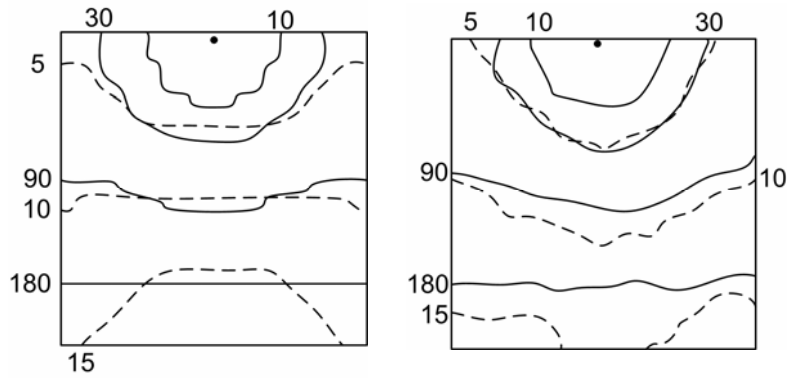


Figure 7: Results for regular (L) and irregular (R) cell distribution

The results for regular and irregular cell distribution are shown in figure 7; they do not differ greatly, from which it follows that for a more complex geometry the cells may be arbitrarily positioned, but still as evenly as possible.

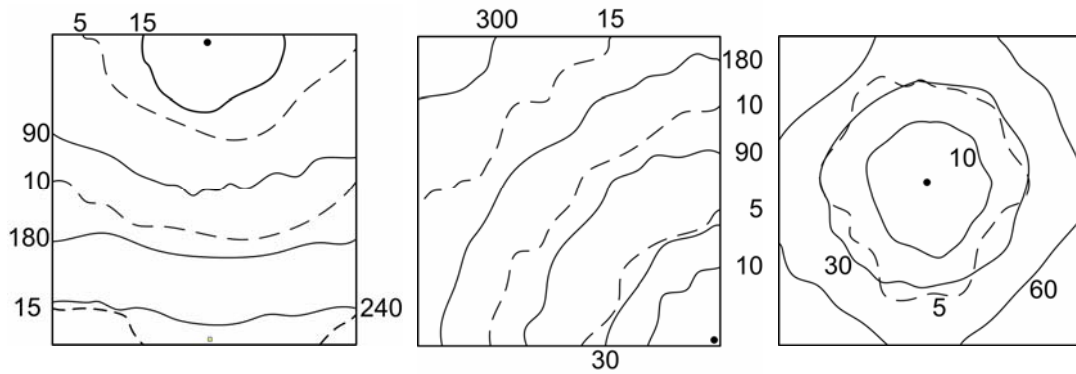


Figure 8: The effect of altering the injection point (the black spot)

The effect on the filling time is clearly to be seen in figure 8. Essentially, it is possible to place the inlet anywhere, but as with actual injection, the mould fills considerably faster with a central inlet than with one in the corner. The model also allows for injection from multiple inlets at different locations, opened at different times.

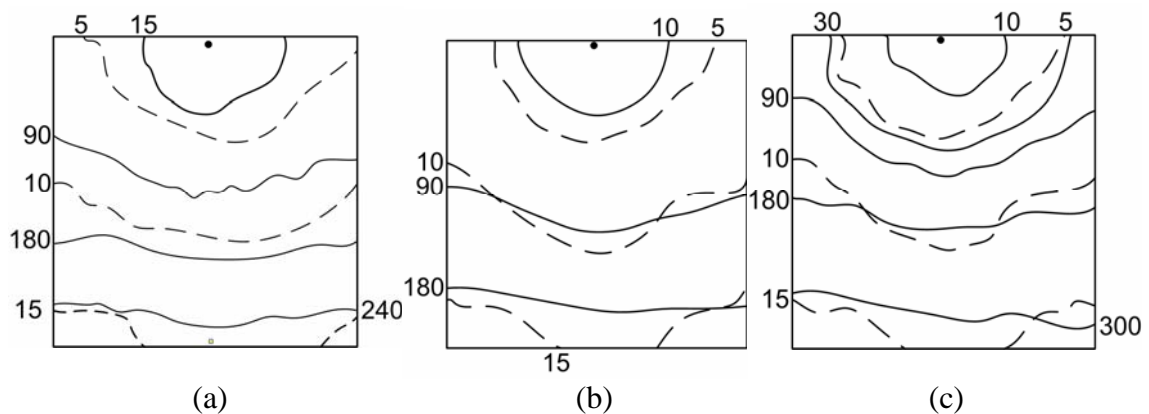


Figure 9: Effect of varying the inlet pressure. (a) normal, (b) halved (c) doubled

As Figure 9 shows, after the same number of calculation steps the flow front is further advanced at double than at normal pressure but develops in much the same way.

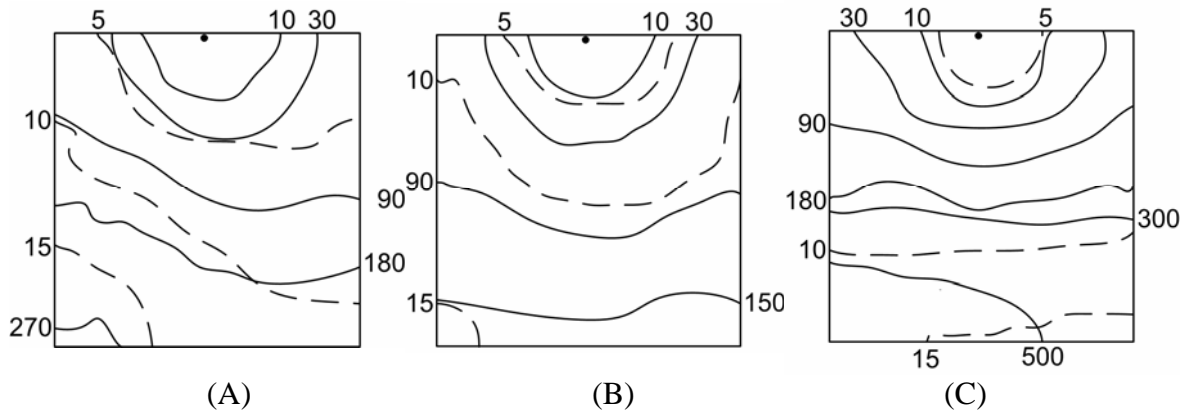


Figure 10: Effect of varying the cell density (A) falling left to right, (B) falling top to bottom (C) rising top to bottom.

When the cell density is altered, the filling pattern changes substantially (Figure 10). The filling front also develops differently, advancing significantly more slowly where the cell density is higher.

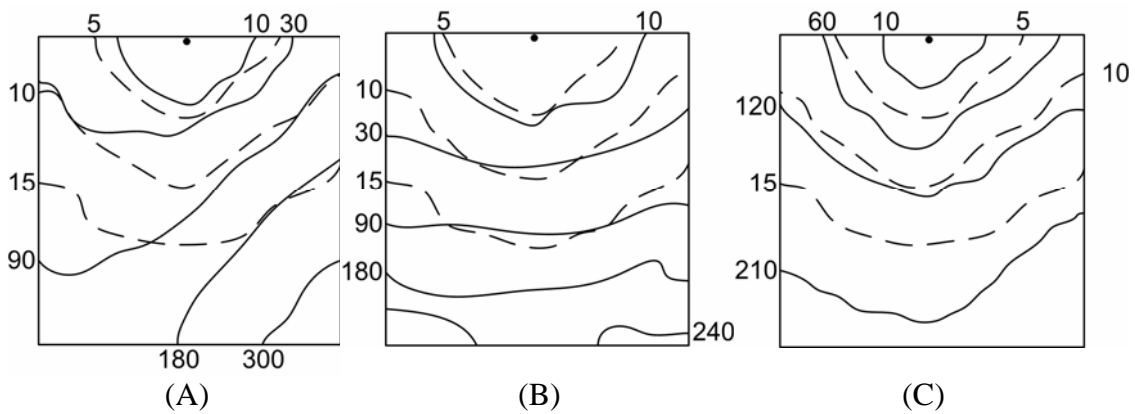


Figure 11: Effect of varying the permeability (A) falling left to right, (B) falling top to bottom (c) rising top to bottom.

The more rapid advance of the filling front in regions of higher permeability is clearly to be seen in Figure 11.

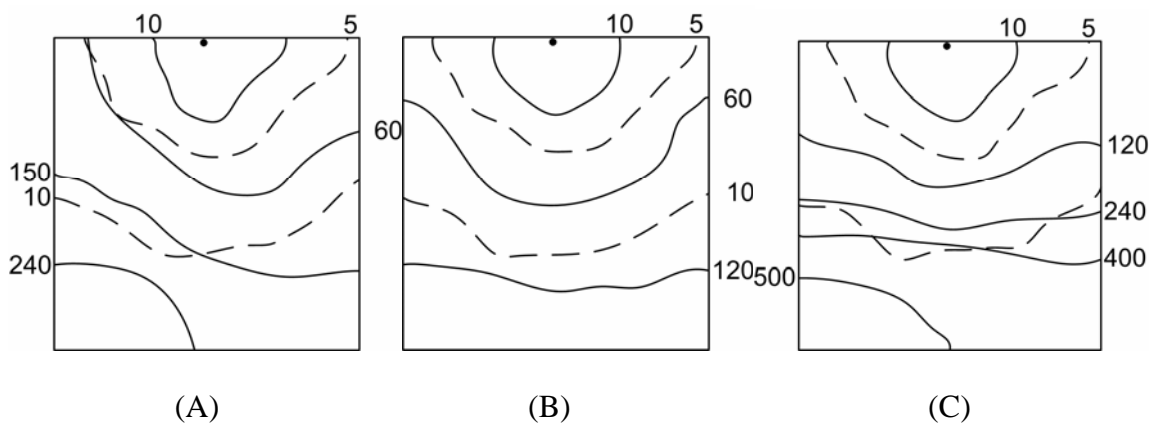


Figure 12: Effect of varying the porosity (A) falling left to right, (B) falling top to bottom (B) rising top to bottom.

The slower advance of the filling front in regions of higher porosity is clearly to be seen in Figure 12.

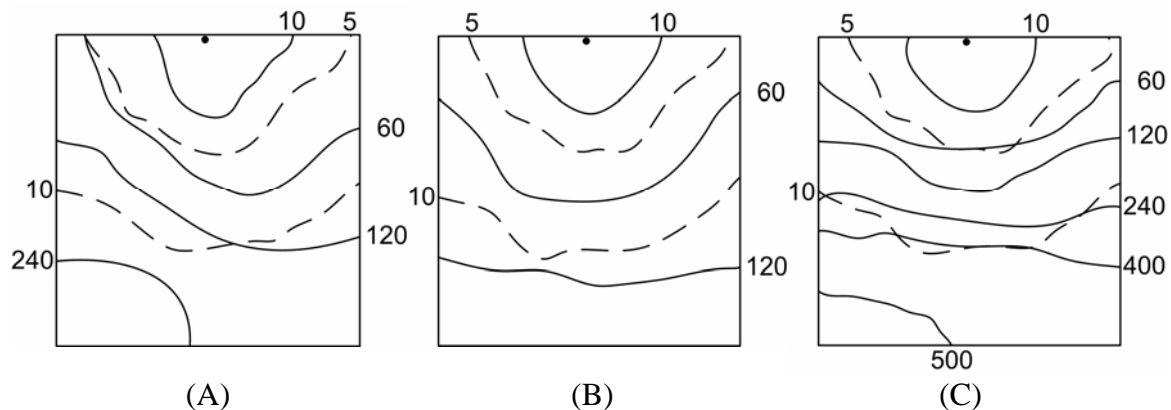


Figure 13: Effect of varying the height of the cavity (A) falling left to right, (B) falling top to bottom (C) rising top to bottom.

Altering the cavity height also significantly affects the flow pattern, as Figure 13 shows. This effect is also observed in practice.

In principle the cellular automaton using the proposed algorithm correctly represents the filling process. The predicted effects on the filling behaviour of varying the sprue position and pressure, permeability, porosity and cavity height all agree qualitatively with those observed in practice.

The dependency of the filling behaviour on the cell spacing needs to be improved, as the results shown in Figure 10 demonstrate. It will certainly be possible to correct it by adjusting the weighting factors in the algorithm or by modifying the algorithm itself.

#### 4. Conclusions and future Outlook

The simulation of LCM processes using cellular automats is in principle possible.

The algorithm developed in this work correctly describes the behaviour during mould filling in a qualitative way, but requires further refinement. The chief difficulties are in dealing with different cell densities, and in the high pressure drop at the inlet.

The first few runs of the calculation are decisive for a correct description of the filling process. For this reason it is desirable to improve and refine the modelling of the inlet and the early stages of injection. It is also of interest to extend the model to allow for more than one injection point.

In order to be able to make quantitative predictions of the evolution of the filling process the time step needs to be further investigated, and the resulting predictions compared with corresponding measured values from testing.

In parallel with the latter, the expected improved results should be compared with those from FEM simulation and the advantages of the method set out.

#### 5. Acknowledgements

The work described here was financed by the Werner Steiger Foundation.

This support made it possible to carry into practice the idea of simulating the RTM process by means of cellular automats, and the authors hereby acknowledge it with grateful thanks.

## **Literature**

- [1] M. Hintermann, Erforschung eines neuen Injektionsprozesses für offene und geschlossene Faserverbund- Strukturen, Dissertation ETH Nr. 12522, 1998
- [2] Klaus Richter und Jan-Michael Rost, Komplexe Systeme, Fischer Taschenbuch Verlag, ISBN 3-596-15550-9